The mechanical response of a PBX and binder: combining results across the strain-rate and

frequency domains

The mechanical response of a PBX and binder: combining results across the strain-rate and frequency domains

D R Drodge[1,4]**, D M Williamson**[1]**, S J P Palmer**[1]**, W G Proud**[2] **and R K Govier**[3]

[1] SMF Group, Cavendish Laboratory, University of Cambridge, CB3 0HE, UK
[2] Institute of Shock Physics, Imperial College London, SW7 2AZ, UK
[3] AWE Aldermaston, Reading, RG7 4PR, UK

E-mail: daniel.drodge@eng.ox.ac.uk

Abstract

The mechanical response of a polymer bonded explosive (PBX) has been measured using a Split Hopkinson Pressure Bar at a strain-rate of $2000\,\text{s}^{-1}$, across a range of temperatures from 173 to 333 K, with the aim of observing its behaviour in the glassy regime. The yield stresses increased monotonically with decreasing temperature and no plateau was found. The failure mechanism was found to transition from shear-banding with crystal debonding fracture to brittle failure with some evidence of crystal fracture. Similar experiments were performed on samples of its nitrocellulose-based binder material, at a strain-rate of $3000\,\text{s}^{-1}$ across a temperature range 173–273 K. The failure stresses of the binder approach that of the composite at temperatures near $-70\,^\circ\text{C}$. The elastic moduli were estimated from post-equilibrium regions of the stress–strain curves, and compared with those obtained for the composite using 5 MHz ultrasonic sound-speed measurement, and powder dynamic mechanical analysis measurements and quasi-static behaviour reported in a previous paper. The moduli were plotted on a common frequency axis: a temperature shift was applied to collapse the curves, which agreed with the Cox–Merz rule.

(Some figures in this article are in colour only in the electronic version)

1. Introduction

A polymer bonded explosive (PBX) is typically a particulate composite of organic crystals in a polymer matrix, filled to volume fractions of 60% to 80%. PBX design and subsequent handling are strongly influenced by the need to reduce their sensitivity, i.e. the tendency for explosive initiation to result from accidental stimuli such as flame or impact. In the case of impact-loading, the immediate concerns are of localized heating through friction, adiabatic pore collapse or shear-banding, which can lead to critical hot-spot formation [1]. Furthermore, microstructural damage can occur, increasing the risk of initiation resulting from further impact or exposure to

flame [2]. Underlying a good understanding of PBX impact sensitivity, and underpinning any mechanical modelling of these materials, is the study of their mechanical properties at a range of strain-rates and temperatures. Much research has been performed into the underlying microstructural causes [3].

The PBX studied here is a composite of the secondary explosive HMX (cyclotetramethylene-tetranitramine) and NC-K10, a mixture of nitrocellulose and a combination of plasticizing agents known as K10. This particular binder differs from others such as HTPB or estane, being a non-crosslinked polymer mixture. It exhibits fluid properties at high temperatures and low strain-rates, and has been observed to leach from the composite over long periods of time [4]. The HMX crystals have a bimodal particle-size distribution, with the coarser particles of sizes around 90 μm and finer particles around 10 μm [4]. The explosive accounts for 91% of the

---

[4] Address for correspondence: Department of Engineering Science, Parks Road, University of Oxford, OX1 3PJ.

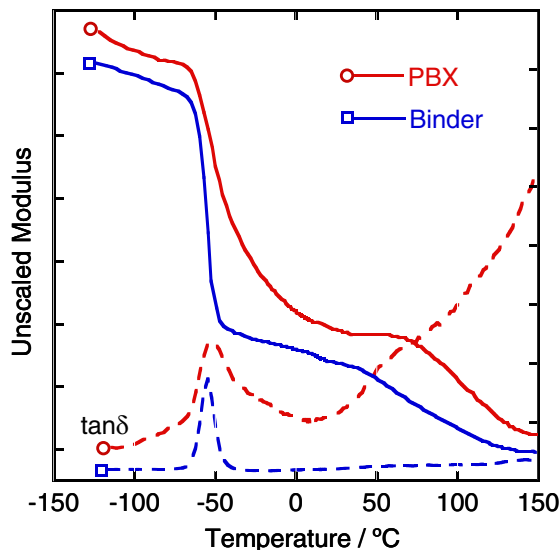J. Phys. D: Appl. Phys. **43** (2010) 335403

D R Drodge *et al*

Figure 1. 1 Hz powder-DMA temperature-span for the PBX and its binder. Modulus and tan δ scales are arbitrary.

mass of the composite, which is consolidated from a moulding powder of binder-wetted HMX by isostatic pressing at elevated temperature. The resulting material has negligible porosity.

A significant study of the rate- and temperature-dependence of its compressive strength is reported by Williamson *et al* [5]. The authors' main achievement was to obtain data spanning a range of 130 K in temperature and ten decades of strain-rate and map the two variables using the time–temperature equivalence principle. He rejected the Williams–Landel–Ferry form [6] in favour of a logarithmic conversion between strain-rate and T, which was shown to provide a better fit to the data. The conversion is of the form

$$\Delta T = S \log(\dot{\varepsilon}_1/\dot{\varepsilon}_2),$$

where $\dot{\varepsilon}_1$ and $\dot{\varepsilon}_2$ are the strain-rates. The shift factor obtained was $S = 13.1 \pm 0.2$ K per decade of strain-rate. Williamson later performed Brazilian disc indirect tension experiments at quasi-static rate over a range of temperatures, finding again that a similar linear conversion factor was applicable [7].

Dynamic mechanical analysis (DMA) thermal-scan experiments were also performed, albeit in a limited form that does not generate quantitative values of the moduli. Specifically, the experiments were performed on shavings made of a PBX specimen, placed in an aluminium jacket. This, rather than a standard DMA experiment on a higher mass rod-shaped specimen, was necessary for safety reasons. Figure 1 shows the results at a driving frequency of 1 Hz, along with those of the binder. Although the curves are arbitrarily scalable, they do show the locations of transitions and indicate their relative sharpness.

Williamson *et al* used a fixed temperature of 22 °C when compressing the material at various strain-rates, and a fixed rate of 10^{-3} s^{-1} for the temperature-spanning experiments. His results indicate a constant strain-to-failure in both cases, a trend noted in other PBXs by Wiegand [8]. This forms the basis for the argument that it is valid, under the theory of linear

viscoelasticity, to treat yield stress as an equivalent function of both T and $\dot{\varepsilon}$. If failure always occurs at strain ε_f irrespective of $\dot{\varepsilon}$ or T, then σ_y will be approximately proportional to the Young's modulus, E. Hence σ_y becomes a means of investigating the viscoelastic behaviour of the composite.

Of course, as previous authors have noted, this depends on the constancy of ε_f, and the analogy with linear viscoelasticity is not strictly valid due to the strains being finite. Furthermore, the consequences of the composite nature of the material are not accounted for: for example, the dependence of mechanical properties upon damage or effects of strain localizing in the binder phase. This extension of Williamson's study is intended to probe conditions under which the elastic modulus of the binder approaches that of the filler (in this case, 15.2 GPa for HMX [9]).

The first measurements taken were estimates of a high-frequency elastic modulus, calculated from ultrasonic sound speeds, measured across a narrow temperature range, using 5 MHz transducers. The next set of experiments were compression-to-failure, for a temperature-span at fixed strain-rate, this time at 2000 s^{-1}. Similar Split Hopkinson Pressure Bar (SHPB) experiments on the PBX have been reported by other researchers [10], albeit for fewer temperature points, with no modulus estimation and no study of the binder in isolation.

2. Ultrasonic measurements

2.1. Method

Ultrasonic transducer probes were used in a two-probe 'send and receive' mode. A control module excites a pulse in the sender probe, and amplifies any signals detected by the receiver probe, producing a periodic trace that can be monitored on an oscilloscope [11]. The time lag from the incident pulse to the point of initial rise of the received pulse is deemed to be the travel time. Both shear and longitudinal transducers were used for these experiments, which were conducted in a steel bomb-box. Experiments were performed on five 1 inch^2 slabs of the PBX, of thicknesses ranging from 3.2 to 15.2 mm. Sound speed was calculated by finding the gradient of specimen thickness against time lag.

Thermal control was achieved by passing hot or cold nitrogen gas into the bomb-box. The gas was heated using an electrical heating element and cooled using a heat-exchange coil immersed in a liquid nitrogen bath. The volume of the bomb-box is very large compared with the size of the specimen, so a small wooden sub-chamber was built around the apparatus to reduce the thermally controlled volume. Temperature was monitored at the point of gas inflow and at the surface of the specimen. According to the probe manufacturer, exposure to low or high temperatures may cause delamination of the piezoelectric element. At temperatures lower than −5 °C, the probe signals began to manifest electrical spiking, so the experiments were stopped.

2.2. Results

Ultrasonically measured sound speeds are shown in figure 2. The errors shown are those arising from the estimation of the
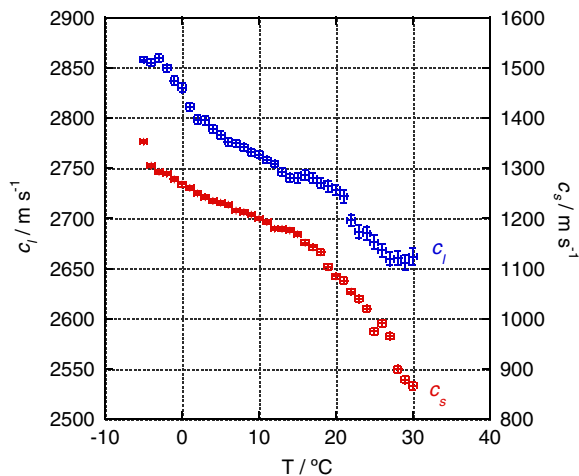
Figure 2. Shear and longitudinal sound speeds, c_l and c_s, measured using 5 MHz ultrasonic probes on samples of five different thicknesses.
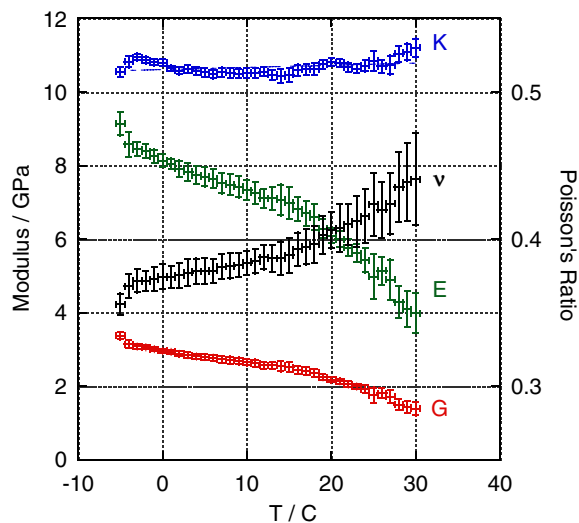

Figure 3. Elastic properties derived from sound speeds, measured using 5 MHz ultrasonic probes.

gradient. A room-temperature material density of $1841 \pm 2\,\mathrm{kg\,m^{-3}}$ is assumed, based on a previous paper [5]. The derived elastic modulus, E, bulk modulus, K, shear modulus, G, and Poisson's ratio, ν, are plotted against temperature in figure 3.

3. SHPB measurements

3.1. Method

A 12.7 mm diameter Inconel SHPB (described in [12]) was used for these experiments. The striker bar length was 200 mm and the input and output bars were 500 mm long with semiconductor strain gauges mounted at the midpoints. Gray advises the use of Inconel steel bars for experiments at non-ambient temperatures [13]. Despite the relatively high impedance of these bars compared with the PBX and its binder, equilibrium should not be significantly hindered, as established by Siviour *et al* [14]. Pulse-shapers, in the form of 0.2 mm thick
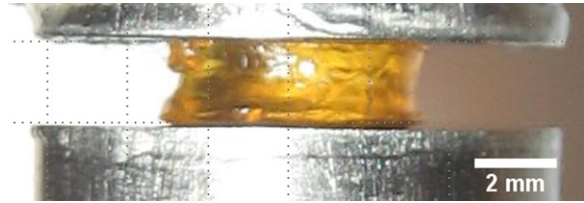

Figure 4. Photograph of binder disc, between the bars. The bar diameter, 12.7 mm, acts as a scale for measuring the specimen dimensions.

annealed copper shim, were placed on the striker-facing end of the input bar to prevent the formation of oscillations in the loading pulses (see, e.g., [15]), the main aim being to ensure the validity of some of the pre-yield stress–strain data.

An environmental chamber, into which cooled or heated nitrogen gas was piped, was used for specimen temperature control during these experiments. A K-type thermocouple was attached to the Inconel output bar and used as the measure of experiment temperature. The bar ends were lubricated with a thin layer of silicone grease, chosen because of its low glass-transition temperature.

Machined specimens of the PBX were supplied by AWE, as discs of 8.0 mm diameter and 3.2 mm thickness. NC-K10 binder was supplied in the form of sheets of about 1 mm in thickness. Two such sheets were overlaid and left overnight at room temperature to fuse together. A 5 mm diameter punch was used to cut cylindrical samples from this sheet. These specimens were placed between the lubricated bar ends, and the bars were brought together, compressing the specimen to a thickness of approximately 2 mm. A photograph was taken of the specimen between the bars, from which its length and diameter could be estimated, using the bar diameter to calibrate for scale (see figure 4). The photograph was taken using telephoto zoom from a stand-off of 2 m to reduce barrel distortion. After photographing the specimen, the environmental chamber was put in place without disturbing the bars.

Both types of specimens were compressed at a range of temperatures. As the number of PBX specimens was limited, no repeat measurements were performed. Two additional experiments were made, one at room temperature and one at $-70\,^{\circ}\mathrm{C}$, with a strain-interrupting aluminium ring placed around the specimens to limit the load to 3% strain for subsequent inspection.

3.2. Results

Stress–strain curves for the PBX are shown in figure 5. The stress–strain curves obtained for the binder are shown in figure 6. Due to the roughness of the sample edges, the diameters of the samples are ill-defined, measurable only to an accuracy of 0.1 mm.

Photographs of the PBX specimens before and after interrupted compression at two temperatures are shown in figure 7. Environmental scanning electron microscope (ESEM) images of the fracture surfaces from specimens compressed in the interrupted-strain experiments are shown in figure 8.
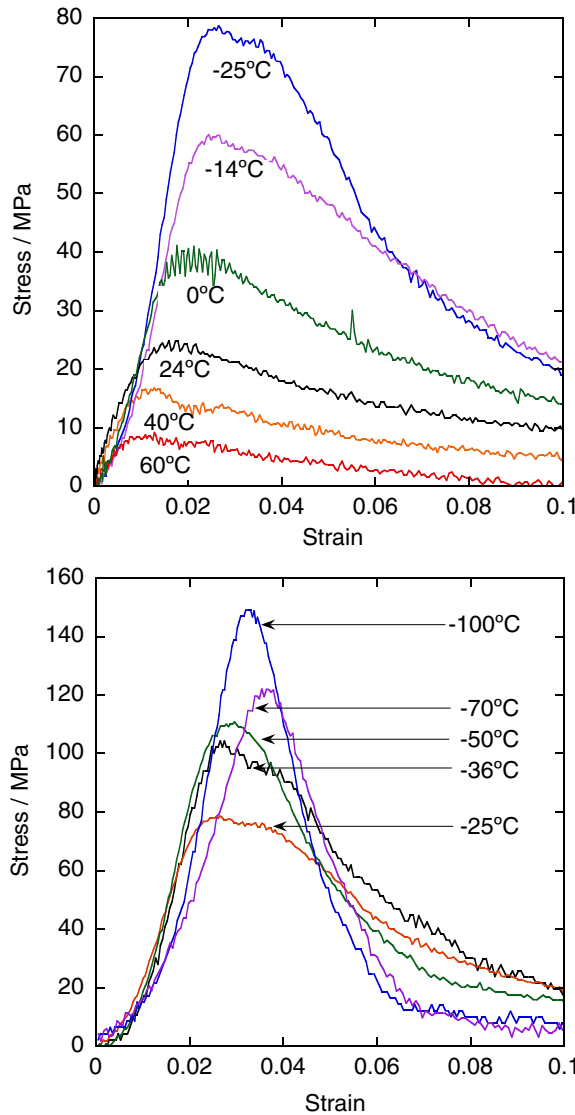
Figure 5. Stress–strain curves for the PBX at nominal strain-rates of 2000 s⁻¹, across a range of temperatures: (*a*) 60 to −25 °C (*b*) −25 to −100 °C.

Figure 6. Stress–strain curves for the binder at nominal strain-rates of 3000 s⁻¹, over a range of temperatures: (*a*) 0 to −60 °C (*b*) −60 to −100 °C, including repeats.

The failure stresses of the PBX and binder are plotted against temperature in figure 9, alongside the SHPB results obtained by Govier *et al* [10] and Williamson's quasi-static PBX data [5]. The error-bars shown on the plots are estimated from the noise level at the peak of the respective stress–strain curve. Below the apparent glass-transition region, the binder exhibits no failure peak as such, so the stress at which flow begins is taken to represent material strength.

4. Discussion

The ultrasonically measured elastic properties span quite a small temperature range (0 to 30 °C) compared with the SHPB curves (−100 to 60 °C). A trend of decreasing shear and Young's modulus with increasing temperature is clear from figure 3, and expected given the DMA response of the material at a lower frequency (figure 1). The scale of modulus variation, i.e. from 4 to 9 GPa in the Young's modulus, is very large,
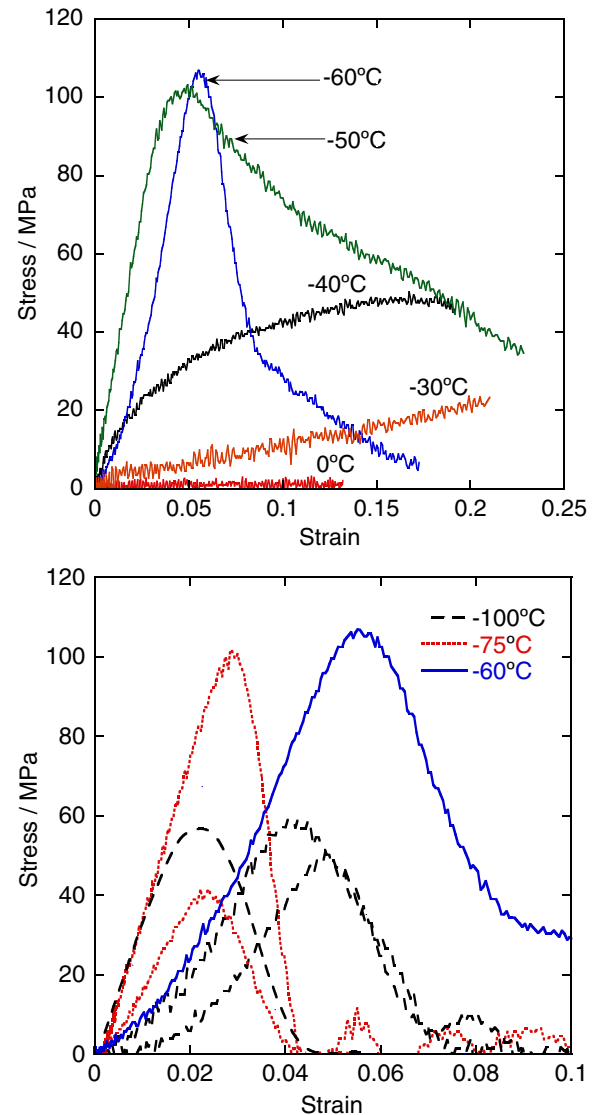
implying that a major transition is underway. This could be the glass transition seen in the DMA data, measured at a different temperature due to the higher operating frequency used by this technique.

Turning to the SHPB results, it appears that the variation of strength with temperature appears similar in form to the strength-temperature data obtained in [5] at quasi-static strain-rates. A glass-transition region is seen in both cases, at around −60 °C quasi-statically and −30 °C using the Hopkinson bar, implying that the increase in strain-rate has had a similar effect to reducing the temperature. Figure 10 reproduces figure 9 with the quasi-static data translated using Williamson's predicted 13.1 °C shift per decade of strain-rate. The shifted points occupy broadly the same trend as the SHPB points, although the point at 50 °C would appear to be higher than the shifted data, understandable given the high level of noise.

The time–temperature behaviour is as expected for a viscoelastic material. Unlike idealized viscoelastic behaviour
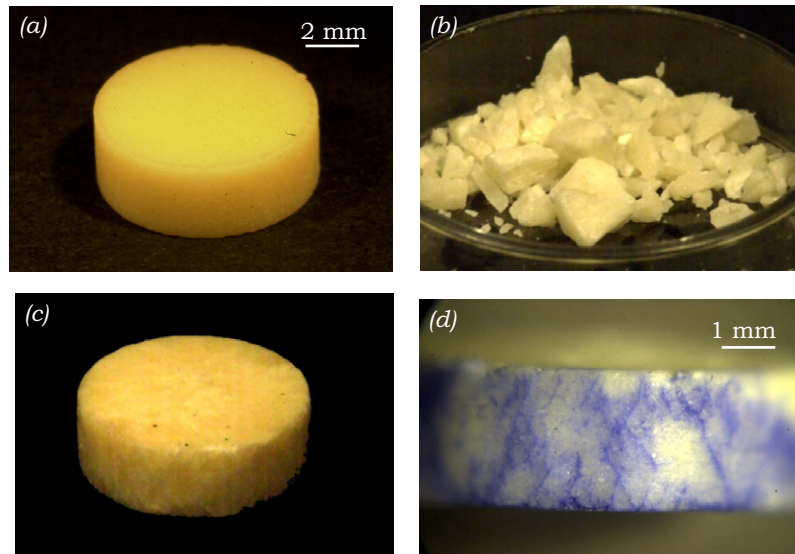
Figure 7. Photographs of PBX specimens (*a*) undamaged; (*b*) compressed to 3% strain at −70 °C; (*c*) compressed to 3% strain at 22 °C; (*d*) same specimen as figure (*c*), stained with blue dye to illustrate shear-banding. Scale shown in (*a*) also applies to (*b*) and (*c*).
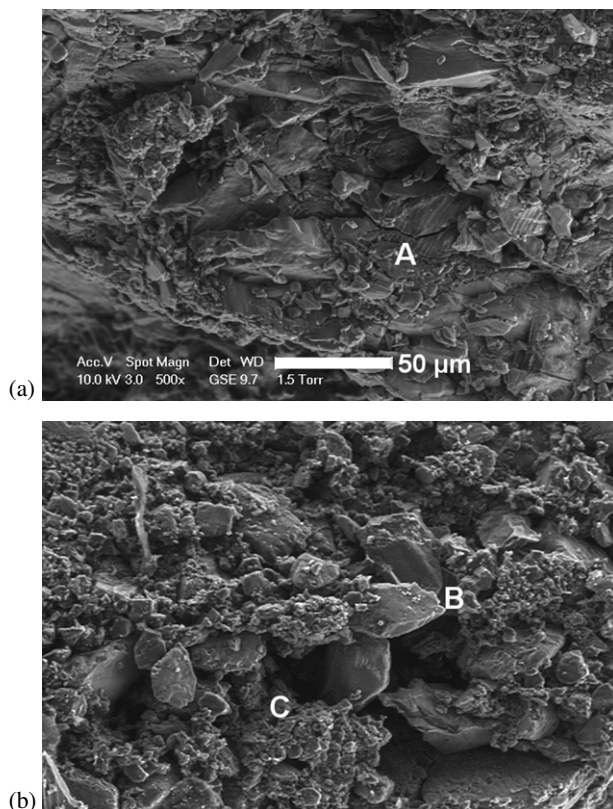

Figure 8. ESEM images showing fracture surfaces of the PBX after recovery from SHPB compression. (*a*) Sub-T_g specimen (0 °C) showing crystal fracture at 'A'. (*b*) Super-T_g specimen showing a protruding grain at 'B' and a recess at 'C', along with less exposed crystal surface than figure 8(*a*), implying adhesive failure. The scale shown in (*a*) also applies to (*b*).

Figure 9. Plot of PBX and binder failure stresses against temperature, including *quasi-static data from [5] and **SHPB data from [10].

there is no glassy plateau of constant failure stress for either the PBX (in which the strength increases) or the binder (in which the strength decreases with significant variation between repeats)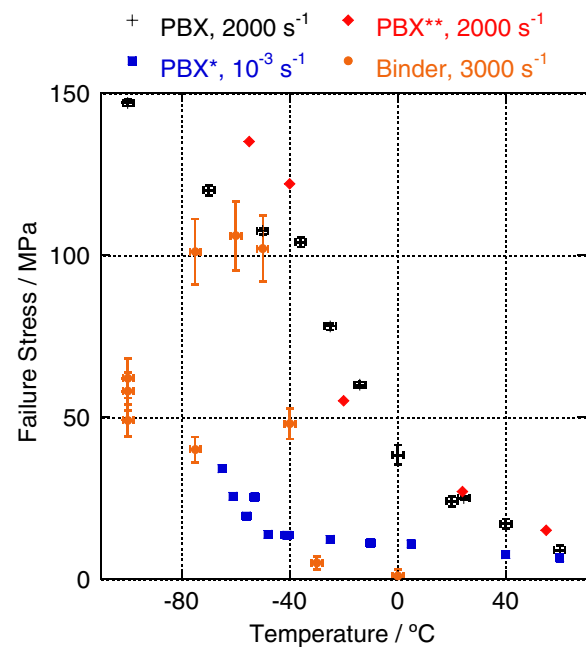. This is because the true viscoelastic mechanical response profile is expressed in terms of a storage modulus, not the strength. Below T_g, we note a change in the form of the stress–strain curves from the strain-softening form typical of PBX materials to that more indicative of sudden brittle failure.

This change in behaviour is consistent with electron micrographs obtained of post-failure Brazilian disc specimens, where sub-T_g fracture occurs through the crystals rather than around them [4, 16]. Inspection of post-failure specimens bears this out, as shown in figure 7. The room-temperature specimen has failed through shear-banding, as has previously
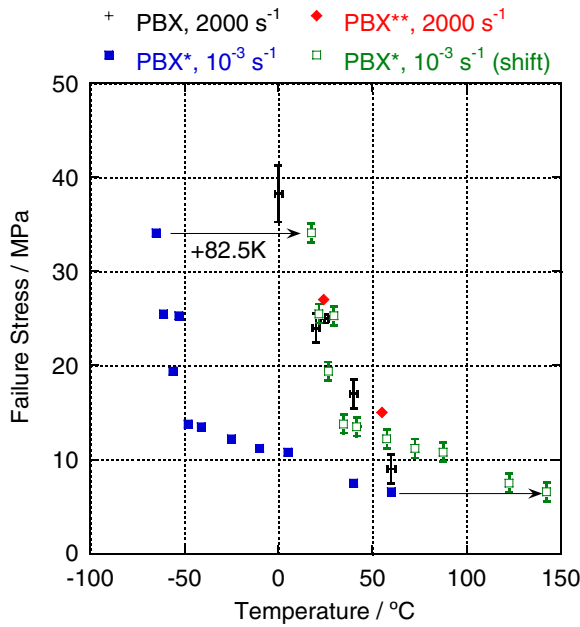
Figure 10. Enlargement of figure 9, with the quasi-static data presented in [5] shifted by log $R = 82.5\,°C$, where $S = 13.1\,K$ is the shift factor and $R = 2 \times 10^6$ is the ratio of SHPB to quasi-static strain-rates.
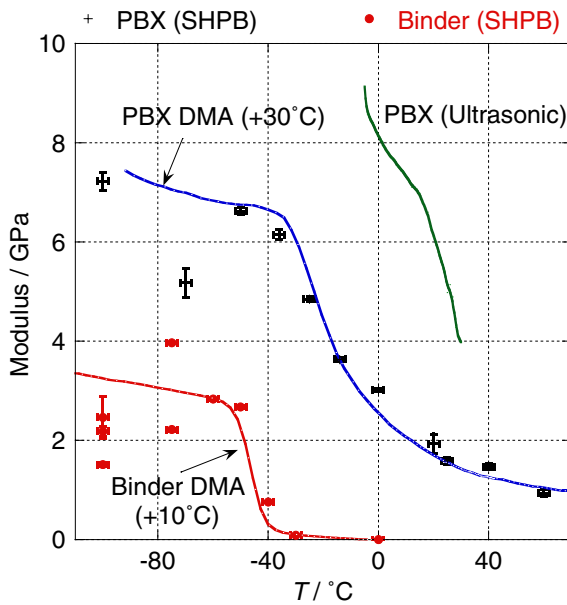

Figure 11. Plot of PBX and Binder 'SHPB pseudo-modulus' against temperature, alongside the PBX Young's modulus from figure 3. The DMA curves from figure 1 are included—their modulus values have been rescaled and temperature-shifted to fit the SHPB moduli shown. The binder DMA required a shift of $+10\,°C$ and the PBX DMA required a shift of $+30\,°C$.

been observed in quasi-static compression [17]. ESEM images taken of representative specimens are shown in figure 8: the $-75\,°C$ image (figure 8(*a*)) shows large amounts of flat, exposed crystal; whereas the $0\,°C$ image (figure 8(*b*)) shows more rounded crystals and roughened surface. The former is believed to be a sign of brittle crystal fracture, the latter of debonding.

4.1. Elastic moduli

To obtain a 'pure' master curve for these materials, the storage (i.e. elastic) modulus must be obtained from the SHPB stress–strain curves. The post-equilibrium, pre-yield gradients were used to estimate the modulus. Equilibrium was assessed by comparing the 1-wave and 2-wave force records, as explained in [13]. A plot of PBX and binder elastic moduli, as well as the PBX ultrasonic Young's modulus, against temperature, is shown in figure 11. Some of the curves used to estimate modulus had varying gradients prior to yield. In these cases, the steepest and shallowest gradients were used as upper and lower bounds. In other cases the error in modulus is simply that of the gradient. The unscaled powder-DMA curves from figure 1 are overlaid to illustrate the similarity in their shape, with a shift in the temperature axis as shown.

The PBX modulus appears, aside from the points at -70 and $-75\,°C$, to follow the expected shape, with what looks like a plateau in modulus at low temperatures. The ultrasonically measured values span a similar range of values, but imply a continued increase in E as temperature falls. This may be due to a fault in ultrasonic probe performance at low temperatures. Alternatively, it may be an accurate portrayal of the material properties, and the SHPB experiments not representative of this trend due to the lack of repeats, despite the good correlation with the rescaled DMA curves.

The binder moduli trace the beginnings of a glass-transition region before displaying scatter. We have assumed that the scatter in failure stress was due to brittle failure occurring at the glassy plateau. However, if we have reached a plateau, the modulus should remain constant despite the variations in the failure stress. The scatter and slight decline at decreasing temperature may be due to the build-up of internal stresses in the specimens due to thermal contraction. Given the rough edges on the specimens, contraction would produce stress concentrations at flaws on the sample faces, weakening them. Significant contraction in the specimen length and diameter implies overestimation of all specimen dimensions. This would lead to the underestimation of strain to the first power and stress to the second, so modulus will be underestimated to the first power.

There are two important differences between the shapes of the PBX and binder SHPB (and DMA) modulus–temperature curves, shown in figure 11. Firstly, the glass transition appears to occur at a lower temperature in the binder. Secondly, the jump in modulus is much steeper in the binder. This may be explained by considering the micromechanical strain-rate experienced by the composite.

The PBX binder, which occupies just 20% of the composite volume, is less stiff than the filler crystals so will undergo almost all the deformation in the specimen. If the global specimen deformation is ε, the regions of binder must undergo strains higher than this, depending on its local thickness, which we may well assume is not uniform. The binder in a composite specimen therefore experiences a range of strain-rates, all of them higher than the composite strain-rate; whereas a specimen of pure binder experiences a single strain-rate. The glass transition seen in the PBX SHPB results in figure 11 is actually that of the binder experiencing a range of

J. Phys. D: Appl. Phys. **43** (2010) 335403

D R Drodge *et al*

higher strain-rates than the $2000\,s^{-1}$ quoted for the composite. The binder glass transition is that of the binder at a single rate of $3000\,s^{-1}$. As a result the composite transition is shifted to a higher temperature, and being representative of a range of deforming binder thicknesses (hence strain-rates), shows a less well-defined increase.

The modulus data have a further possible use in investigating the relationship between strain-rate and frequency. As the SHPB data have a known rate and the ultrasonic and DMA data have known frequencies, their relative shifts can be used. The shift required to move the DMA curve to overlay the SHPB points for PBX was +30 K. Combining this with the shift from SHPB to ultrasound, of approximately +50 K, gives a total shift of 80 K, corresponding to a frequency shift from 1 Hz to 5 MHz. The implied linear conversion is 11.9 K per decade of frequency, which is quite close to that obtained previously [5]. The implied frequency of the SHPB experiments is 320 Hz. Applying the Cox–Merz rule to this we obtain an equivalent strain-rate of $2040\,s^{-1}$, which matches the typical strain-rates seen in the SHPB experiments.

5. Conclusions

The mechanical properties of a UK PBX formulation were measured across a range of temperatures, with the goal of expanding the existing range of data to include low-temperature, high strain-rate glassy behaviour. Ultrasonic transducers were used to measure the high-frequency elastic properties in the temperature range from -5 to $30\,°C$. SHPB experiments were also performed on the PBX and its binder at a variety of temperatures ranging from -100 to $60\,°C$. The observed pattern in failure strains confirms, and expands upon, that seen in quasi-static data by Williamson *et al* [5] and supports a strain-rate temperature shift factor of 13.1 K per decade.

The use of pulse-shaping allowed estimation of the elastic modulus from SHPB stress–strain curves; the pattern seen matched that observed in Williamson's DMA data. Differences between PBX and binder modulus–temperature curves may be explained by the range of binder thicknesses present in a composite specimen. Superposition of unscaled DMA-measured moduli with ultrasonically measured Young's moduli produces a frequency-temperature shift factor of 11.9 K per decade. Applying this shift, and using the Cox–Merz rule, recovers the SHPB strain-rate from the DMA frequency.

This implication, that frequency-temperature shifts can be mapped to a strain-rate-temperature perspective, warrants further investigation given the inherent usefulness of strain-rate dependent, as opposed to frequency-dependent, parameters when coding finite-element simulations.

References

[1] Field J E 1992 *Acc. Chem. Res.* **25** 489
[2] Berghout H L, Son S F, Skidmore C B, Idar D J and Asay B W 2002 *Thermochimica Acta* **384** 1–2
[3] Walley S M, Siviour C R, Drodge D R and Williamson D M 2010 *JOM J. Miner. Met. Mater. Soc.* **62** 1
[4] Rae P J, Goldrein H T, Palmer S J P, Field J E and Lewis A L 2002 *Proc. R. Soc. Lond. Ser.* A **458** 743–62
[5] Williamson D M, Siviour C R, Proud W G, Palmer S J P, Govier R, Ellis K, Blackwell P and Leppard C 2008 *J. Appl. Phys. D: Appl. Phys.* **41** 085404
[6] Williams M L, Landel R F and Ferry J D 1955 *J. Am. Chem. Soc.* **77** 3701–7
[7] Williamson D M, Palmer S J P, Proud W G and Govier R K 2009 Brazilian disc testing of a UK PBX approaching the glass transition temperature *Shock Compression of Condensed Matter*; *AIP Conf. Proc. (Nashville, TN)* (New York: AIP) **1195** 803–6
[8] Wiegand D 2003 *J. Energ. Mater.* **21** 109–24
[9] Banerjee B 2004 *Int. J. Solids Struct.* **41** 481–509
[10] Govier R K, Gray G T III and Blumenthal W R 2008 *Metall. Mater. Trans.* A **39** 535–538
[11] Arnold N D and Guenther A H 1966 *J. Appl. Polym. Sci.* **10** 731–43
[12] Gama B A, Lopatnikov S L and Gillespie J W 2004 *Appl. Mech. Rev.* **57** 223–50
[13] Gray III G T 2000 Classic split Hopkinson bar testing *ASM Handbook—Mechanical Testing and Evaluation* vol 8 (Materials Park, OH: ASM International) pp 463–76
[14] Siviour C R, Walley S M, Proud W G and Field J E 2001 Are low impedance Hopkinson bars necessary for stress equilibrium in soft materials? *New Experimental Methods in Material Dynamics and Impact* (Warsaw: Institute of Fundamental Technological Research) pp 421–7
[15] Follansbee P S and Frantz C 1983 *J. Eng. Mater. Technol.* **105** 61–6
[16] Williamson D M, Palmer S J P and Proud W G 2007 Brazilian disc testing of a UK PBX below the glass transition temperature *Shock Compression of Condensed Matter*; *AIP Conf. Proc. (Waikoloa, HI)* (New York: AIP) **955** 803–6
[17] Williamson D M 2006 Deformation and fracture of a polymer bonded explosive and its simulants *PhD Thesis* Cambridge University